Nat Hazards
DOI 10.1007/s11069-016-2331-z

ORIGINAL PAPER

Wind-wave prediction equations for probabilistic offshore hurricane hazard analysis

Vahid Valamanesh[1] · Andrew T. Myers[1] · Sanjay R. Arwade[2] · Jerome F. Hajjar[1] · Eric Hines[3] · Weichiang Pang[4]

Received: 10 December 2015 / Accepted: 15 April 2016

Abstract The evaluation of natural catastrophe risk to structures often includes consideration of uncertainty in predictions of some measure of the intensity of the hazard caused by the catastrophe. For example, in the well-established method of probabilistic seismic hazard analysis, uncertainty in the intensity measure for the ground motion is considered through so-called ground motion prediction equations, which predict ground motion intensity and uncertainty as a function of earthquake characteristics. An analogous method for evaluating hurricane risk to offshore structures, referred to herein as probabilistic offshore hurricane hazard analysis, has not been studied extensively, and analogous equations do not exist to predict offshore hurricane wind and wave intensity and uncertainty as a function of hurricane characteristics. Such equations, termed here as wind and wave prediction equations (WWPEs), are developed in this paper by comparing wind and wave estimates from parametric models with corresponding measurements during historical hurricanes from 22 offshore buoys maintained as part of the National Data Buoy Center and located near the US Atlantic and Gulf of Mexico coasts. The considered buoys include observations from 27 historical hurricanes spanning from 1999 to 2012. The 27 hurricanes are characterized by their eye position, translation speed, central pressure, radius to maximum winds, maximum wind speed, Holland B parameter and direction. Most of these parameters are provided for historical hurricanes by the National Hurricane Center's H*Wind program. The exception is the Holland B parameter, which is calculated using a best-fit procedure based on H*Wind's surface wind reanalyses. The formulation of the WWPEs is based on two parametric models: the Holland model to estimate hurricane winds and Young's model to estimate hurricane-induced waves. Model predictions are

✉ Andrew T. Myers
atm@neu.edu

[1] Department of Civil and Environmental Engineering, Northeastern University, Boston, MA 02215, USA

[2] Department of Civil and Environmental Engineering, UMASS Amherst, Amherst, MA 01003, USA

[3] Department of Civil and Environmental Engineering, Tufts University, Medford, MA 02155, USA

[4] Glenn Department of Civil Engineering, Clemson University, Clemson, SC 29634, USA

Published online: 27 April 2016

made for the 27 considered historical hurricanes, and bias and uncertainty of these predictions are characterized by comparing predictions with measurements from buoys. The significance of including uncertainty in the WWPEs is evaluated by applying the WWPEs to a 100,000-year stochastic catalog of synthetic hurricanes at three locations near the US Atlantic coast. The limitations of this approach and remaining work are also discussed.

Keywords Probabilistic offshore hurricane hazard analysis · Hurricane risk · Uncertainty quantification · Offshore structures

List of symbols

B	Pressure profile exponent (i.e., the Holland B parameter)
F_X	Cumulative probability density function of random variable X
GMPE	Ground motion prediction equation
L	Fetch length
MRP	Mean return period
P_c	Hurricane central pressure
P_n	Ambient pressure
PGA	Peak ground acceleration
PGV	Peak ground velocity
POHHA	Probabilistic offshore hurricane hazard analysis
PSHA	Probabilistic seismic hazard analysis
R_{max}	Hurricane radius of maximum wind speed
R'	Effective hurricane radius
S_a	Spectral acceleration
V_g	Sustained 10-min wind speed at gradient level
V_{max}	Hurricane maximum wind speed
V_{tr}	Hurricane translation speed
WWPE	Wind and wave prediction equation
d	Water depth
f_X	Probability density function of random variable X
f_c	Coriolis parameter
g	Acceleration due to gravity
r	Radial distance measured from the center of the hurricane eye
x	Variable representing modeled environmental intensities (e.g., sustained 1-min wind speed at 10-m elevation V or significant wave height H_s)
x_c	Variable representing bias-corrected modeled environmental intensities (e.g., bias-corrected sustained 1-min wind speed at 10-m elevation V_c or bias-corrected significant wave height $H_{s,c}$)
$\hat{x}$	Variable representing measurements or probabilistic realizations of environmental intensities (e.g., sustained wind speed $\hat{V}$ or significant wave height $\hat{H}_s$)
$\bar{y}$	Vector of parameters characterizing a hurricane at a particular instant
Φ	Standard normal cumulative probability distribution function
ε_X	Normally distributed random variable representing the difference between the logarithms of measured and modeled values for X. Positive values correspond to measured values greater than modeled values
θ	Hurricane direction angle measured relative to north (clockwise positive)
μ	Mean

v	Annual rate of occurrence
ρ	Air density
σ	Standard deviation

1 Introduction

The concept of probabilistic offshore hurricane hazard analysis (POHHA) originated in response to probabilistic seismic hazard analysis (PSHA), which was first proposed by Cornell in 1960 (Cornell 1964, 1968). PSHA has evolved significantly over the past several decades since its inception and is currently a widely used method for designing and evaluating risk to structures exposed to seismic hazard. An integral component of PSHA is the ground motion prediction equation (GMPE) which predicts ground motion intensity (e.g., peak ground acceleration or spectral acceleration) and its uncertainty as a function of earthquake characteristics (e.g., magnitude, site-to-source distance). Such equations are usually developed empirically based on hundreds to thousands of measurements of ground motion intensity. In contrast to PSHA, POHHA and its onshore counterpart have received considerably less research attention, and equations analogous to GMPEs do not exist to predict offshore hurricane wind and wave intensity and uncertainty as a function of hurricane characteristics.

The open literature relevant to hurricane risk has frequently considered potential hurricane activity probabilistically, using a stochastic catalog of synthetic hurricanes (e.g., Russell 1971; Tryggvason et al. 1976; Batts et al. 1980; Georgiou et al. 1983; Georgiou 1985; Neumann 1991; Vickery and Twisdale 1995; Vickery et al. 2000a; Vickery and Wadhera 2008a) to augment the $\sim$150-year historical record of Atlantic hurricane activity and provide tens of thousands of probabilistic realizations of 1 year of potential hurricane activity. Risk assessments based on such catalogs usually require the estimation of hazard intensity measures for each realization of a hurricane in the catalog. In most cases, these relationships have been modeled deterministically (e.g., Holland 1980; Huang et al. 2001; Young 1988), although there have been several exceptions (e.g., Vickery et al. 2009a, b, c; Jayaram and Baker 2010) which consider uncertainty in the relationship between hurricane realizations and the sustained wind speed. The study by Vickery et al. (2009a, b, c) found that uncertainty in the Holland model could be characterized with a coefficient of variation of 10 %. The study by Jayaram and Baker (2010) found that, after correcting for an observed bias, uncertainty in the Batts wind field model could be modeled with a normally distributed random variable with zero mean and standard deviation of 15 %, representing the difference between the logarithms of predicted and measured values. For offshore applications, however, no researchers have focused on evaluating uncertainty in the relationship between hurricane realizations and wave and few have considered wind. In summary, the literature has produced no systematic relationships to account for uncertainties in the prediction of offshore wind speed and wave height for assessing hurricane risk to offshore structures. Such relationships, termed here as wind and wave prediction equations (WWPEs), are developed in this paper. These equations are developed by first identifying historical Atlantic hurricanes and buoys for which measurements of wind and wave during hurricanes are available, then using two parametric models to estimate hurricane-induced sustained wind speed and significant wave height for these hurricanes and buoy locations, then comparing the predicted values with measurements and finally using

statistical analysis to characterize biases and uncertainty in the predicted values, thereby providing equations which can estimate bias-corrected wind and wave during hurricanes including estimates of uncertainty.

This paper starts by presenting a general formulation of POHHA that is consistent with the well-established method of PSHA. Following this, the paper details the availability of buoy measurements of wind and wave during historical hurricanes and then lists the specifications of these hurricanes. Next, the paper describes two parametric models: the Holland (1980) model to estimate sustained wind speeds and Young's (1988) model to estimate the significant wave height during hurricanes. The predictions of these parametric models are compared with buoy measurements, and a formulation of the WWPEs is presented including consideration of biases and uncertainty. It is noted that this approach, which starts with parametric models and then uses empiricism to identify biases and uncertainty in these models, is distinct from that used in the original development of GMPEs, which was based entirely on regression-based empiricism. The paper concludes by demonstrating the use of WWPEs through numerical examples at three sites off the coasts of Massachusetts, Delaware and Georgia. The examples are based on a 100,000-year stochastic catalog of synthetic hurricanes (Liu 2014). At each of the three sites, sustained

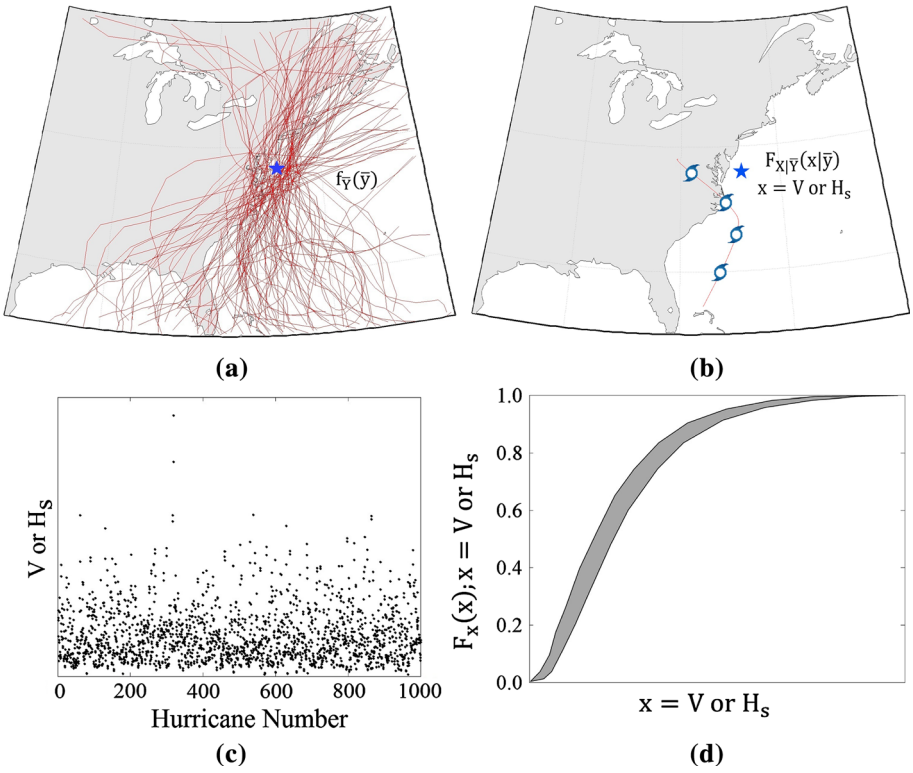

Fig. 1 Overview of the key steps of probabilistic offshore hurricane hazard analysis including **a** assessment of hurricane hazard through synthetic hurricane tracks from a stochastic catalog of hurricanes, **b** prediction of wind V or wave H_s using WWPEs for each synthetic hurricane, including uncertainty, **c** generation of realizations of V or H_s for each hurricane event and **d** development of a CDF for each realization of V or H_s

wind speeds and significant wave heights are calculated for several mean return periods (MRPs) to assess the significance of including uncertainty in the WWPEs.

2 Formulation of POHHA

The objective of POHHA is to estimate a probability distribution for the recurrence of intensities of the sustained wind speed and significant wave height at a particular offshore location. Based on this distribution, probabilities of exceedance and MRPs can be calculated for particular values of the intensity. The mathematical formulation of POHHA is shown generically as,

$$F_X(x) = \int F_{X|\bar{Y}}(x|\bar{y}) f_{\bar{Y}}(\bar{y}) \mathrm{d}\bar{y} \tag{1}$$

where $F_{X|\bar{Y}}(x|\bar{y})$ is the conditional cumulative probability distribution function for a random variable $X = x$ representing wind or wave intensity conditioned on random vector $\bar{Y} = \bar{y}$, $f_{\bar{Y}}(\bar{y})$ is the probability density function of $\bar{Y}$, X is a random variable representing wind or wave intensity, $\bar{Y}$ is a vector of parameters characterizing a hurricane, and $F_X(x)$ is the cumulative distribution function of random variable X.

This paper is focused on the development of WWPEs, which are represented in Eq. (1) as $F_{X|\bar{Y}}(x|\bar{y})$. The WWPEs probabilistically estimate random variable X, where X is equal to either V, the 1-min sustained wind speed at an elevation of 10 m, or H_s, the significant wave height, as a function of hurricane parameters $\bar{Y}$. The parameters considered in the vector $\bar{Y}$ for the numerical example in this paper are eye position, central pressure, maximum wind speed, radius to maximum wind speed, hurricane translation speed, hurricane translation angle and the Holland B parameter. Since the location and characteristics of a hurricane are not stationary in time, the distribution of hurricane parameters $f_{\bar{Y}}(\bar{y})$ is considered here through a stochastic catalog of synthetic hurricane events, which characterizes the hurricane parameters $\bar{Y}$ at regular intervals over the duration of the hurricane. The stochastic catalog is, in effect, a discrete set of realizations of $f_{\bar{Y}}(\bar{y})$ that is calibrated to be consistent with the historical record and understanding of the physics governing hurricanes. The POHHA procedure is illustrated schematically in Fig. 1, with the WWPEs represented in Fig. 1b.

3 Buoy measurements of wind and wave during hurricanes

In this study, wind and wave measurements during hurricanes are obtained from the National Data Buoy Center (NDBC) which is a part of the National Oceanic and Atmospheric Administration (NOAA). The NDBC maintains 67 buoys located off the Atlantic coast and Gulf of Mexico of the USA. Many of these buoys provide hourly (and in some cases semi-hourly) measurements of sustained wind speed (averaged over 8 min) at a 5-m elevation above the sea surface and significant wave height (averaged over 20 min); however, many other buoys provide only wind or wave measurements. Some buoys also provide additional data, such as average wave period, dominant wave period, wind direction and atmospheric pressure; however, this work considers only measurements of the wind speed and significant wave height.

From these 67 buoys in the NDBC network, a subset of 22 is considered here. This subset is selected based on data availability, specifically that the buoy must have

simultaneously measured both wind speed and significant wave height and the buoy must be located near the track of at least one historical hurricane. The geographic distribution of the 22 buoys is shown in Fig. 2, and the buoy specifications are listed in Table 1. The stations are divided into four categories based on water depth, *d*; slightly less than half (47 %) of the buoys are located in water depths less than 60 m, and 11 % of the buoys are located in water depths less than 30 m.

From these 22 buoys, a total of 62 measurements of wind and wave during hurricanes are available. Of these 62 observations, seven are missing data before the end of the hurricane. In these situations, a procedure is employed wherein the missing data are evaluated relative to results from a 30-year hindcast provided by the National Center for Environmental Protection (NCEP). The study combines winds from Climate Forecast System Reanalysis (CFSR) with waves modeled with WAVEWATCH III to provide a coupled reanalysis of metocean conditions from 1979 to 2009 (Saha et al. 2010; Chawla et al. 2013). As an illustrative example of the situation where the CFSR/WAVEWATCH III results are used, Fig. 3 shows wind speed measurements from NDBC buoys compared to the CFSR/WAVEWATCH III hindcast results for three buoy locations during hurricane Floyd in 1999. The figure shows that, for Buoys 41008 and 41009, there is no interruption in the measurements of the wind data, and, in these cases, the CFSR/WAVEWATCH III results are not used. However, for Buoy 41004, measurements are missing during the period when the wind speed was expected to reach a peak value. In this case, the peak value is estimated, as shown in the figure, using an analysis of the ratio of the CFSR/WAVEWATCH III results to the buoy measurements for peak conditions during other hurricanes.

4 Characterization of historical hurricanes

The tracks and characteristics of historical hurricanes are taken from the H*Wind project (Powell et al. 1998), which uses observations and models to provide parameters characterizing historical hurricanes, specifically the central pressure, radius of maximum winds,

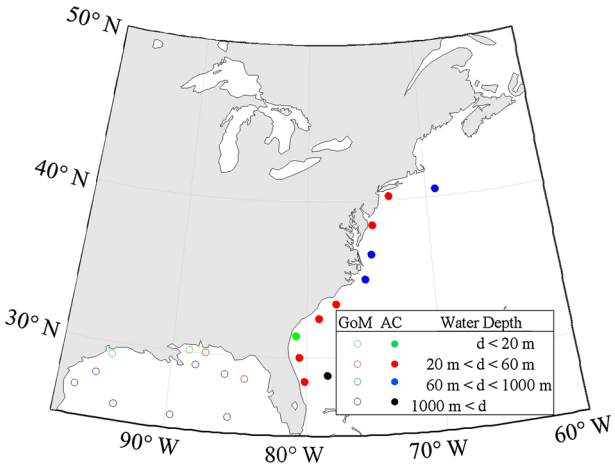

Fig. 2 Locations and water depths of 22 NOAA buoys considered in this study. *d* Water depth, *GoM* Gulf of Mexico, *AC* Atlantic coast

Table 1 Specifications of the NDBC buoys considered in this study

Category	NOAA station ID	Latitude	Longitude	Dist. to shore (km)	Water depth (m)	Observation length (years)	Number of measurements
Shallow ($d < 20$ m)	41008*	31.40°N	80.87°W	35	20	21	3
	42007	30.10°N	88.77°W	10	15	29	3
	42035	29.23°N	94.41°W	29	13	21	2
Medium (20 m $< d <$ 60 m)	44025	40.25°N	73.16°W	45	40	28	1
	44009*	38.46°N	74.70°W	31	31	29	1
	41013	33.44°N	77.74°W	50	24	9	3
	41004	32.50°N	79.10°W	66	38	23	4
	42012	30.06°N	87.55°W	22	28	5	1
	41012	30.04°N	80.53°W	74	38	11	3
	41009	28.52°N	80.19°W	35	41	25	5
	42036	28.50°N	84.52°W	136	51	20	1
Deep (60 m $< d <$ 1000 m)	44008*	40.50°N	69.25°W	102	66	31	1
	44014	36.61°N	74.84°W	96	95	23	4
	41025	35.01°N	75.40°W	28	68	10	4
	42040	29.21°N	88.21°W	75	165	19	3
	42039	28.79°N	86.01°W	118	274	19	3
	42019	27.91°N	95.35°W	96	83	24	2
	42020	26.97°N	96.69°W	67	80	24	1
Very deep (1000 m $< d$)	41010	28.90°N	78.46°W	202	1873	25	7
	42002	26.09°N	93.76°W	336	3125	37	1
	42003	26.04°N	85.61°W	320	3274	38	5
	42001	25.89°N	89.66°W	331	3365	37	4
Total							62

* Buoy considered in the numerical example provided in Sect. 9

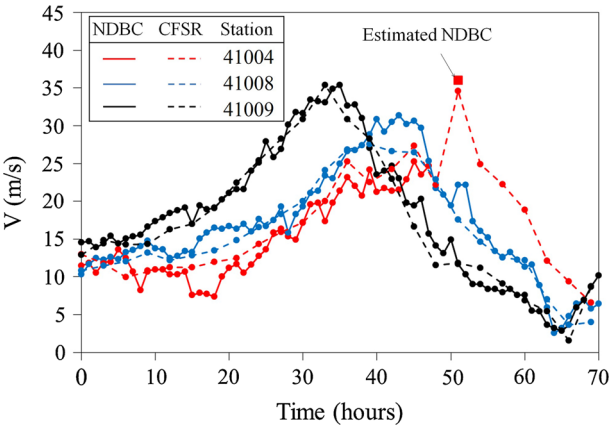

Fig. 3 NDBC buoy measurement and CFSR/WAVEWATCH III results for three NDBC buoy locations during Hurricane Floyd in 1999. Buoy 41004 is missing data during the hurricane, and, in this study, the missing data are estimated using the CFSR/WAVEWATCH III results as shown

maximum wind speed and eye position of historical hurricanes at 3- to 6-h intervals. The translation speed and direction are calculated based on the eye position. At each time interval, the H*Wind project also provides the 1-min sustained wind field at 10 m above the surface on a rectangular grid. Using these results along with the available buoy measurement data (see Table 1), a set of 27 historical hurricanes occurring between 1999 and 2012 is selected for this study. The selection is based on the proximity of a historical hurricane's track relative to NDBC buoys. Specifically, hurricanes with tracks that are further than 250 km from any of the considered buoys are excluded. Another filter is then applied to remove low-intensity hurricanes with maximum wind speeds measured at the buoy lower than 20 m/s. The paths of the 27 hurricanes are illustrated in Fig. 4, and key characteristics of each hurricane are listed in Table 2. One hurricane parameter, which is

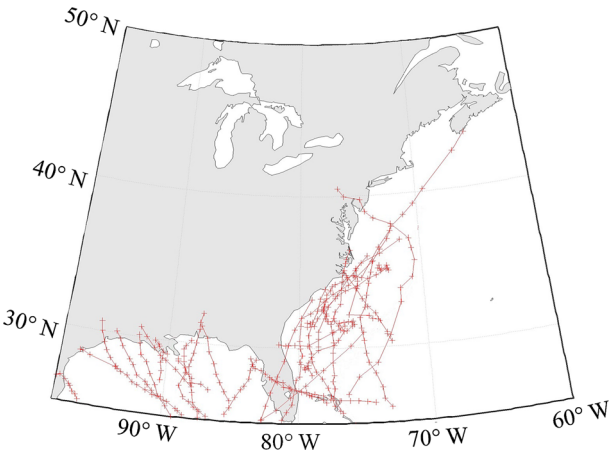

Fig. 4 Twenty-seven historical hurricane tracks considered in this study occurring between 1999 and 2012. Markers indicate eye positions when data are available from the H*Wind project

Table 2 Characteristics of the 27 historical hurricanes considered in this study

No.	Year	Hurricane	Hurricane category*	Location	# of measurements
1	1999	Floyd	4	AC	3
2	1999	Dennis	2	AC	2
3	1999	Irene	2	AC	2
4	2000	Gordon	2	GoM	2
5	2002	Gustav	TS	AC	1
6	2002	Lili	4	GoM	1
7	2003	Isabel	2	AC	1
8	2003	Claudette	1	GoM	2
9	2004	Ivan	4	GoM	4
10	2004	Jeanne	3	AC–GoM	1
11	2004	Alex	2	AC	4
12	2004	Charley	4	AC–GoM	3
13	2004	Frances	2	AC	5
14	2005	Ophelia	1	AC	7
15	2005	Wilma	3	AC–GoM	2
16	2005	Dennis	4	GoM	2
17	2005	Katrina	5	GoM	4
18	2005	Rita	4	GoM	2
19	2008	Dolly	2	GoM	2
20	2008	Gustav	2	GoM	2
21	2008	Ike	2	GoM	4
22	2009	Ida	1	GoM	3
23	2010	Earl	2	AC	3
24	2011	Irene	1	AC	4
25	2012	Beryl	TS	AC	3
26	2012	Sandy	2	AC	3
27	2012	Isaac	1	GoM	3

AC Atlantic coast, *GoM* Gulf of Mexico, *TS* tropical storm

* Saffir-simpson category based on the maximum 1-min sustained wind speed measured when the hurricane is within the region plotted in Fig. 4

necessary for the present study and is not provided by the H*Wind database, is the Holland B parameter. For this parameter, a value is calculated based on a best-fit procedure using the surface wind fields provided by H*Wind. Details on the best-fit procedure are provided in Sect. 5.1.

5 Parametric models to predict wind and wave during hurricanes

The basis of the WWPEs formulated in this paper are empirical models that predict sustained wind speed and significant wave height based on hurricane parameters. Many models have been proposed to predict wind speed given hurricane parameters (e.g., Kerry

et al. 2006; Vickery et al. 2000b), but there is only one well-known parametric model for predicting hurricane-induced waves (Young 1988). More complex programs are available to model hurricane-induced wind and waves such as ADCIRC (Luettich and Westerink 2004), SWAN (Booij et al. 1999), MIKE21 and the Princeton Ocean Model (Bender and Ginis 2000); however, these models require significant computational resources and are not well suited for the numerical examples presented in this paper which require predictions of wind and wave for thousands of realizations of hurricanes for every considered site. For this reason and for the benefit of making the WWPE formulation easier to implement in practice, two parametric wind and wave models are considered: the wind model proposed by Holland (1980) and revised by Holland et al. (2010) and the wave model proposed by Young (1988). Both models are described in more detail in the following sections.

5.1 The Holland model

In the Holland model, the tangential wind field is given by the pressure field and expressed as,

$$V_g(r) = \left[\frac{B}{\rho}\left(\frac{R_{max}}{r}\right)^B (P_n - P_c)e^{-\left(\frac{R_{max}}{r}\right)^B} + \frac{1}{4}(V_{tr}\cdot\sin(\theta) - r\cdot f_c)^2\right]^{0.5} + \frac{1}{2}(V_{tr}\cdot\sin(\theta) - r\cdot f_c) \quad (2)$$

where V_g is the 10-min averaged gradient wind speed at a radial distance r along from the eye of hurricane, B is the Holland B parameter, R_{max} is the radius of maximum wind speed, V_{tr} is the hurricane translation speed, θ is the angle defining the hurricane translation direction, ρ is air density, P_c is the central pressure, P_n is the ambient pressure, and f_c is the Coriolis parameter (Georgiou 1985). The Holland B parameter represents the shape of the decay of hurricane winds with increasing radial distance from the hurricane eye. This parameter has an important influence on the prediction of wind speeds and is not provided by the H*Wind database. Two approaches for estimating this parameter were applied by Vickery and Wadhera (2008b). In the first approach, the parameter is selected which minimizes the root-mean-square error, where error is defined as the difference between the theoretical central pressure and measured pressure over a range of $0.5R_{max}$–$1.5R_{max}$. The second approach is to select a value of B which matches the maximum wind speed at 10 m predicted by the Holland model with the maximum wind speed from H*Wind. For the present study, spatially distributed measurements of the central pressure are not available for most of the considered hurricanes so a variant of the second method is used to estimate the best B parameter. Specifically, B is selected by minimizing the root-mean-square error between the wind speed predicted by the Holland model and the wind speed provided by H*wind over a range of $0.5R_{max}$–$1.5R_{max}$, with comparisons made at a resolution of roughly 6 km.

Equation 2 provides the gradient wind speed, which, for the present application, is then converted to the surface wind speed at 10 m. Many methods exist to convert the gradient winds to surface winds (Schwerdt et al. 1979; Sparks and Huang 2001), and the approach adopted here is based on results by Powell et al. (2003) who found that the maximum wind speed at 10 m during a hurricane could be estimated as 71 % of the gradient wind speed, averaged over the same duration. Vickery et al. (2000a) showed that for relatively intense hurricanes with no air-sea temperature difference, the typical ratio of surface wind to gradient wind for the maximum wind near the eyewall is between 0.70 and 0.72. For the present application, which seeks to calculate extreme hazard at long MRPs, conversion accuracy is preferred for maximum wind speeds, and for this reason, along with a

preference for a straightforward approach, all surface winds calculated in this study for an elevation of 10 m are assumed to be 71 % of the gradient wind speed,

$$V = 0.71 V_g \tag{3}$$

Conversions between wind speeds with varying time averages are made following the approach proposed by Simiu and Scanlan (1996).

5.2 Young's model

Young's parametric model predicts the spatial distribution of the significant wave height during a hurricane as a function of three hurricane parameters: the radius to maximum winds, the maximum wind speed and the translation speed. The model calculates an equivalent fetch length to account for the situation where the wave speed is comparable to the translation speed of the hurricane. In such a situation, the winds transfer energy to the waves over an effectively longer length, and this effect is represented through an extended, equivalent fetch length. Based on the equivalent fetch length, the significant wave height is estimated using a standard JONSWAP fetch-limited growth relationship. Young used these concepts to create a synthetic database of hurricanes for a range of hurricane parameters and fit the results with a simple model that predicts the spatial distribution of the significant wave height at an instant during a hurricane. Young's equations are summarized below for units in meters and seconds,

$$H_{s,\max} = 0.0016 V_{\max} \left(\frac{L}{g}\right)^{0.5} \tag{4}$$

where g is acceleration due to gravity and L is the equivalent fetch length and defined as

$$L = R'\left(-2.175 \cdot 10^{-3} V_{\max}^2 + 1.506 \cdot 10^{-2} V_{\max} V_{tr} - 0.122 V_{tr}^2 + 0.219 V_{\max} + 0.674 V_{tr} + 0.798\right) \tag{5}$$

where R' is the effective hurricane radius and defined as

$$R' = 22500 \log R_{\max} - 70800 \tag{6}$$

The spatial distribution of the significant wave height H_s is provided by Young through a series of spatial plots specifying the ratio of the significant wave height to the maximum value, $H_{s,\max}$ obtained from Eq. (4).

Young's model was developed for deep water conditions in the open ocean where waves are not influenced by land or the seafloor. The WWPEs developed in this paper are expected to be applied to offshore structures which tend to be located in shallow water, and so, in the following section, the predictions of Young's model are evaluated relative to buoy measurements in shallow water to identify biases in the model.

6 Bias correction and uncertainty quantification in the parametric models

The uncertainty in the WWPEs in this paper is characterized by the residual error ε_X, the difference of the logarithms between buoy measurements $\hat{x}$ and predictions from models x,

$$\varepsilon_X = Ln(\hat{x}) - Ln(x) \tag{7}$$

where the variable x in this paper may be either the sustained wind speed V or the significant wave height H_s. This approach is similar to that in PSHA, where uncertainty in the ground motion intensity measure is usually modeled with the residual error, a normally distributed random variable with zero mean and defined as the difference between logarithms of the measured and modeled ground motion intensity measures (Baker 2013). To provide some context for the numerical meaning of ε_X, it is noted that values of ε_X equal to -0.50 and -0.25 correspond to measured values that are 60 and 78 % of the predicted values, while values of ε_X equal to 0.25 and 0.50 correspond to measured values that are 128 and 165 % of the predicted values. For wind speed, modeled values are determined by the Holland model (see Sect. 5.1), while, for significant wave height, modeled values are determined by Young's model (see Sect. 5.2). Measured values are based on buoy measurements during historical storms (see Sect. 3), and the residual error ε_X is calculated independently for wind and wave based on the maximum measurement and the maximum modeled value during the duration of the hurricane. In the following sections, biases, homoscedasticity and uncertainties of these models are assessed in terms of ε_X.

6.1 Evaluation of biases and homoscedasticity

Two biases were identified and corrected in the residual measure ε_X. The first bias relates to the relationship between ε_V and V, the wind speed as predicted directly by the Holland model. Figure 5 is a scatter plot of ε_V versus V for the 62 available measurements, and the linear regression line of the scatter is superimposed on the figure.

A T test is conducted on the hypothesis that the slope of the linear regression line is zero, and the resulting P value is 1 %. In statistical hypothesis testing, it is common to reject the hypothesis for P values less than 5 %. Based on this convention, the hypothesis is

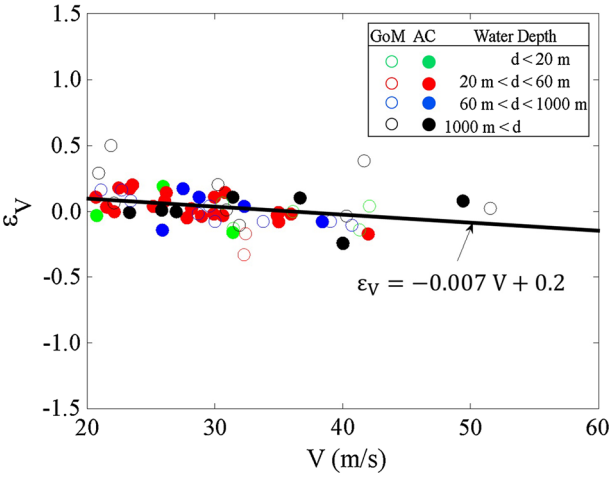

Fig. 5 Scatter plot showing the wind speed residual error ε_V (i.e., the difference of the logarithms of measurements from buoys and predictions from the Holland model) versus V the wind speed predicted by the Holland Model for each of the 62 available measurements. A linear regression line and equation are superimposed. *Marker colors* indicate the water depth at the location of the measurement, and *marker fill* indicates whether the measurement was taken at a location in the Gulf of Mexico or off of the Atlantic coast

rejected here, meaning that the linear bias in ε_V versus V is considered significant. For example, at $V = 20$ m/s, ignoring the bias would mean that predictions of V would be expected to be 94 % of measurements, while at $V = 60$ m/s, predictions of V would be expected to be 124 % of measurements. This is a important difference when considered relative to the variance of ε_V. It is important to note that this observed bias is influenced by the simplistic approach employed here to convert gradient wind speeds to surface wind speeds, see Eq. (3), and it is likely that the bias could be reduced if a more sophisticated conversion method, for example, a boundary layer model or a dynamic numerical model, were used. In this case, a bias-corrected value for the modeled wind speed V_c calculated in terms of the uncorrected value V is expressed as,

$$\ln(\mathrm{V_c}) = -0.007\mathrm{V} + 0.2 + \ln(\mathrm{V}) \tag{8}$$

where both V and V_c are measured in m/s. Based on the bias-corrected prediction of wind speed V_c, a new residual ε_{Vc} is calculated for each observation of the wind speed $\hat{V}$ and the mean value of ε_{Vc} is calculated as 0.00 with a standard deviation of 0.13. Figure 6a–d presents ε_{Vc} and $\varepsilon^2_{V_c}$ versus V_c and the radial position r/R_{max}. Linear regression lines are

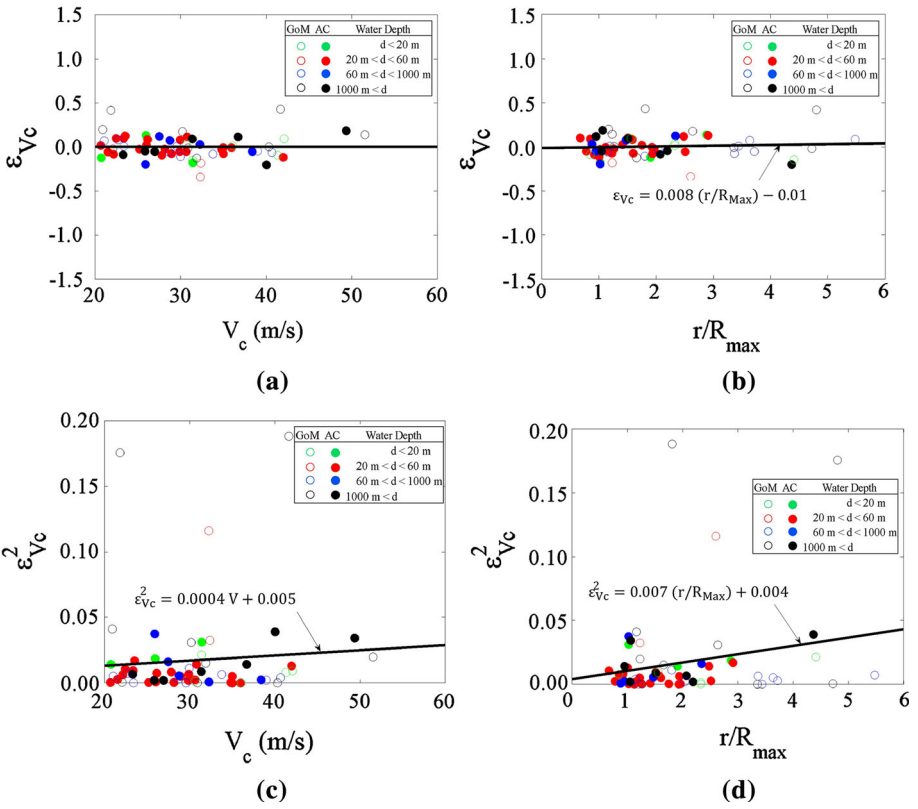

Fig. 6 Evaluation of bias, **a** and **b**, and homoscedasticity, **c** and **d**, for wind speeds estimated by the bias-corrected Holland model and compared to 62 buoy measurements during 27 historical hurricanes. *Marker colors* indicate the water depth at the location of the measurement, and *marker fill* indicates whether the measurement was taken at a location in the Gulf of Mexico or off of the Atlantic coast

superimposed on all four plots. To evaluate the extent of any remaining biases or heteroscedasticity, the slopes of the regression lines are evaluated with a T test, and the results of these tests are provided in Table 3.

A significant bias was also observed in the relationship between ε_{Hs} and the water depth d for shallow water depths. This bias is illustrated in Fig. 7 and is not surprising since Young's model for estimating the significant wave height during hurricanes is developed assuming deep water conditions where the seafloor does not influence the wave height. As shown in the figure, for the measurements considered in this paper, Young's model tends to overestimate the significant wave height in shallow water.

To remove the bias of Young's model with water depth, a bias-corrected value for the significant wave height $H_{s,c}$ is calculated in terms of water depth d and the uncorrected value H_s based on the exponential regression function in Fig. 7 and expressed as,

$$\ln(H_{s,c}) = -e^{-0.06d} + \ln(H_s) \tag{9}$$

where H_s, $H_{s,c}$ and d are measured in meters. Based on the bias correction for the significant wave height, a new residual $\varepsilon_{Hs,c}$ is calculated for each observation of the significant wave height $\hat{H}_s$ and the mean value of $\varepsilon_{Hs,c}$ is calculated as 0.00 with a standard deviation of 0.25. Figure 8a–d presents $\varepsilon_{Hs,c}$ and $\varepsilon^2_{H_{s,c}}$ versus $H_{s,c,}$ and the water depth d with linear regression lines superimposed on all four plots. Note that the horizontal axes of Fig. 8b, d are logarithmic, and thus, the linear regression lines superimposed on these figures appear nonlinear. To evaluate the extent of any remaining biases or heteroscedasticity, the slopes of the regression lines are evaluated with a T test, and the results of these tests are provided in Table 3.

Table 3 provides P values resulting from a T test on the null hypothesis that the linear regression slope of the Y–X data in Figs. 6a–d and 8a–d is zero. Based on the convention in hypothesis testing for rejecting the null hypothesis when P values are less than 5 %, only one of the eight cases in Table 3 is rejected. This particular case relates to the expected value of $\varepsilon^2_{H_{s,c}}$ versus $H_{s,c}$, see Fig. 8c. In this case, the data show that the expected value of $\varepsilon^2_{H_{s,c}}$ decreases with increasing values of $H_{s,c}$. For example, at $H_{s,c} = 5.0$ m, the boundaries

Table 3 Linear regression data and T test results on the statistical significance of the slope of the regression line between the variables listed in the first two columns

Y variable	X variable	Relevant figure	Regression slope (Y/X)	Regression Y-intercept	P value (%)
ε_{Vc}	V_c (m/s)	6a	0 $(m/s)^{-1}$	0	100
ε_{Vc}	r/R_{max}	6b	0.008	−0.01	59
$\varepsilon^2_{V_c}$	V_c (m/s)	6c	0.0004 $(m/s)^{-1}$	0.005	53
$\varepsilon^2_{V_c}$	r/R_{max}	6d	0.007	0.004	9
$\varepsilon_{Hs,c}$	$H_{s,c}$ (m)	8a	−0.02 m^{-1}	0.2	7
$\varepsilon_{Hs,c}$	d (m)	8b	−0.00003 m^{-1}	0.05	20
$\varepsilon^2_{H_{s,c}}$	$H_{s,c}$ (m)	8c	−0.009 m^{-1}	0.1	3
$\varepsilon^2_{H_{s,c}}$	d (m)	8d	−0.00001 m^{-1}	0.07	12

The null hypothesis is that the regression slope is zero. The p value is the probability of observing a slope at least as extreme as the regression slope calculated here given the null hypothesis

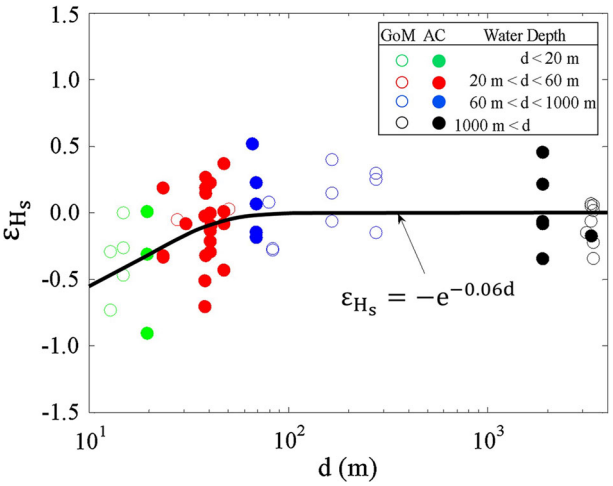

Fig. 7 Scatter plot showing the wind speed residual error ε_{Hs} (i.e., the difference of the logarithms of significant wave height measurements from buoys and predictions from Young's model) versus water depth for each of the 62 available measurements. An exponential regression line and equation are superimposed. *Marker colors* indicate the water depth at the location of the measurement, and *marker fill* indicates whether the measurement was taken at a location in the Gulf of Mexico or off of the Atlantic coast

at plus and minus one standard deviation are 78 and 128 % of the expected value if the bias is ignored, and 74 and 135 % of the expected value if the bias is included. This difference is expected to have a modest influence on the results, and, moreover, a linear bias correction is undesirable because the expected value of the variance would become negative at large but plausible values of $H_{s,c}$. For these reasons, along with a desire to keep the WWPE equations as simple as possible, the linear bias observed in $\varepsilon^2_{H_{s,c}}$ versus $H_{s,c}$ is ignored here. Three other cases are also observed to have small (<20 %) P values: $\varepsilon^2_{V_c}$ versus r/R_{max} (Fig. 6d), $\varepsilon_{Hs,c}$ versus $H_{s,c}$ (Fig. 8a) and $\varepsilon^2_{H_{s,c}}$ versus d (Fig. 8d). In the first case (Fig. 6d), at $r/R_{max} = 4$, the boundaries at plus and minus one standard deviation are 88 and 114 % of the expected value if the bias is ignored, and 83 and 120 % of the expected value if the bias is included. For the second case (Fig. 8a), ignoring the bias at $H_{s,c} = 5.0$ m would mean that predictions of $H_{s,c}$ would be expected to be 95 % of measurements, while at $H_{s,c} = 15.0$ m, predictions of $H_{s,c}$ would be expected to be 105 % of measurements. For the third case (Fig. 8d), at $d = 10$ m, the boundaries at plus and minus one standard deviation are 78 and 128 % of the expected value if the bias is ignored, and 75 and 132 % of the expected value if the bias is included. In all three cases, these biases are ignored in favor a simpler model and because the effect of these biases is modest and the P values associated with these biases are greater than 5 %.

6.2 Uncertainty quantification

The measured distribution of the residual ε_X is plotted with respect to normal distributions with identical means and standard deviations in Fig. 9. Both distributions pass a KS test of normality at 5 % significance; however, it is important to note that the data show that the normality assumption appears to fit worst in the upper tail of the distribution of $\varepsilon_{Hs,c}$. Despite this observation, the normal distribution does reasonably well overall at

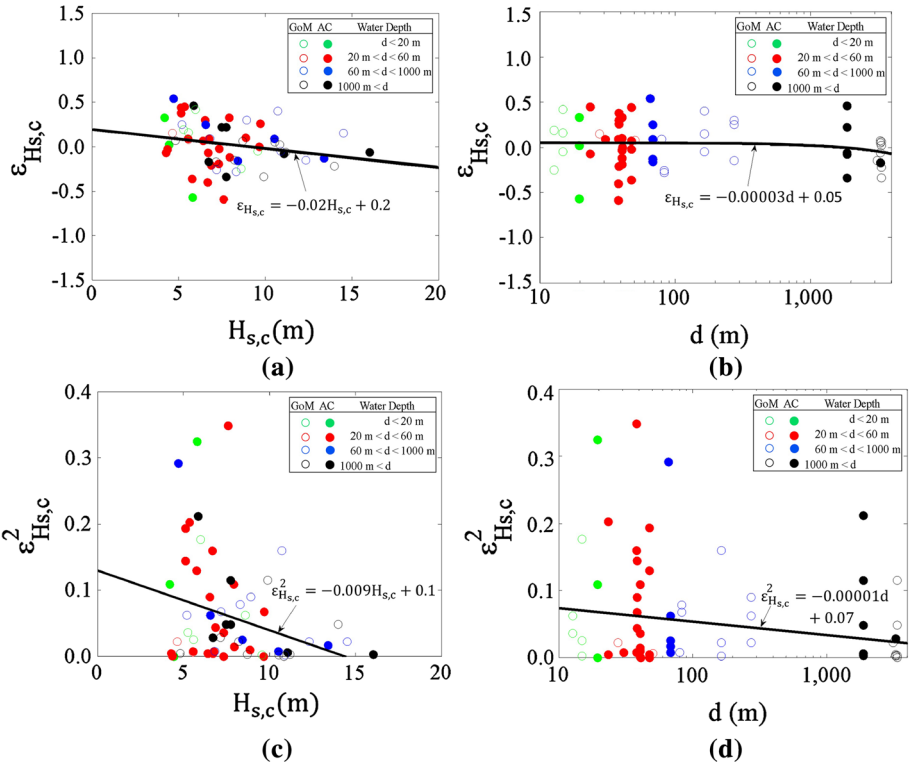

Fig. 8 Evaluation of bias, **a** and **b**, and homoscedasticity, **c** and **d**, for significant wave heights estimated by Young's model and compared to 62 buoy measurements during 27 historical hurricanes. *Marker colors* indicate the water depth at the location of the measurement, and *marker fill* indicates whether the measurement was taken at a location in the Gulf of Mexico or off of the Atlantic coast

Fig. 9 Normality plot for the distribution of ε_{Xc} for $X = H_{s,c}$ and $X = V_c$. *Marker colors* indicate the water depth at the location of the measurement, and *marker fill* indicates whether the measurement was taken at a location in the Gulf of Mexico or off of the Atlantic coast

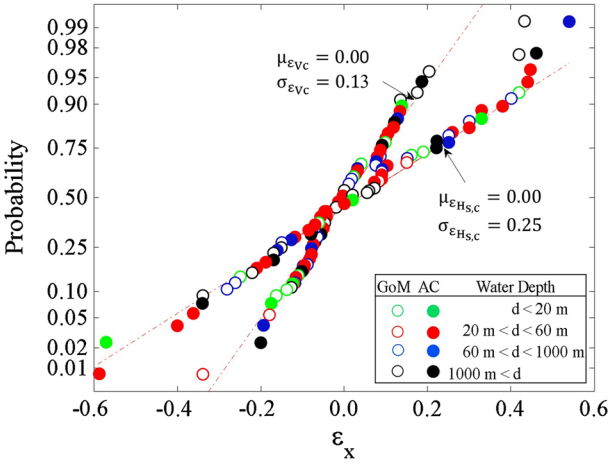

representing the observed values for both ε_{Vc} and $\varepsilon_{Hs,c}$, and this serves as the justification for modeling ε_X as a normally distributed random variable with zero mean and standard deviation equal to 0.13 for V_c and 0.25 for $H_{s,c}$. Both distributions are plotted on logarithmic axes along with the measured data superimposed in Fig. 10.

7 Formulation of WWPEs

Based on the bias correction and uncertainty quantification presented in the previous section, the WWPE for probabilistically estimating the sustained 1-min wind speed at a 10-m elevation is,

$$\hat{V}_c = \exp(\varepsilon_{V_c}) V_c \tag{10}$$

where ε_{Vc} is a normally distributed random variable with zero mean and standard deviation equal to 0.13 and V_c is a bias-corrected prediction of wind speed based on the Holland model (see Eq. 8). The WWPE for probabilistically estimating the significant wave height is,

$$\hat{H}_{s,c} = \exp\left(\varepsilon_{H_{s,c}}\right) H_{s,c} \tag{11}$$

where $\varepsilon_{Hs,c}$ is a normally distributed random variable with zero mean and standard deviation equal to 0.25 and $H_{s,c}$ is a bias-corrected prediction of the significant wave height based on Young's model (see Eq. 9).

8 Limitations of WWPEs

The WWPEs proposed here are formulated using 62 measurements of sustained wind speed and significant wave height during hurricanes from NDBC buoys. Most of the observations correspond to relatively low intensities of wind speed (74 % of the measured

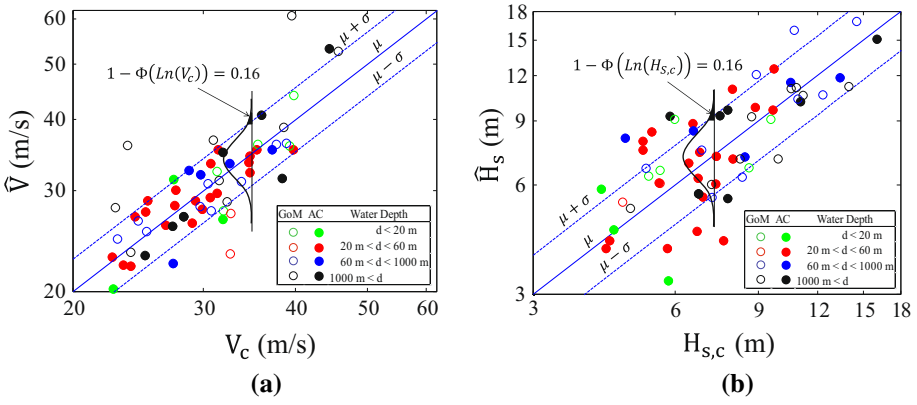

Fig. 10 Probability density function and measured values for **a** bias-corrected wind speed V_c and **b** bias-corrected significant wave height $H_{s,c}$. *Marker colors* indicate the water depth at the location of the measurement, and *marker fill* indicates whether the measurement was taken at a location in the Gulf of Mexico or off of the Atlantic coast

wind speeds are below 35 m/s) and wave height (76 % of the measured wave heights are below 10 m), and more measurements at higher intensities could significantly change the character of the WWPEs. Characterizing the WWPEs at higher intensities is especially important since the hurricane risk to offshore structures is expected to be influenced strongly by intense, but infrequent hurricanes with correspondingly higher wind and wave intensities. Another important limitation in the WWPEs formulated here is that they are derived independently and do not provide any information on the correlation between wind and wave uncertainty. In reality, the wind and wave intensities and their uncertainty are likely correlated to some degree, and this is an important consideration when using these equations to evaluate the hurricane risk to an offshore structure. Moreover, the effect of simultaneity of wind and wave conditions is not considered here since wind and wave conditions are only evaluated separately. Thus, a risk assessment which considered the effect of both wind and wave would ideally somehow account for the fact that it is not likely that the maximum wave height will occur simultaneously with the maximum wind speed at a particular site (Valamanesh et al. 2015).

An additional limitation is that the bias correction for the wind speed was calibrated based on a limited range of wind speed observations (between 20 and $\sim$50 m/s). Beyond this range, the legitimacy of the correction has not been verified and, for very large wind speeds, the magnitude of the bias correction is quite large (e.g., for $V_c = 70$ m/s, the correction in terms of ε_{Vc} is 0.15). The authors do not recommend applying the bias correction to wind speeds significantly outside of the range considered here. Another limitation is that there is no upper bound to the wind speeds and wave heights predicted with the WWPEs. This is particularly important for estimating wave height since it is known that there are physical stability limits to wave height and steepness beyond which a wave will break.

The WWPEs proposed here are based entirely on an empirical formulation, using statistics of simultaneous measurements of wind and wave during hurricanes. Since such measurements are so sparse, the authors recommend that future development and validation of WWPEs incorporate information from dynamic numerical models which use knowledge of the physical laws governing the atmosphere and ocean to supplement the limited availability of measurements.

9 Numerical examples

In this section, examples are provided following the POHHA procedure depicted schematically in Fig. 1 to estimate hurricane wind speeds and significant wave heights at different MRPs using the WWPEs with and without the inclusion of uncertainty. The POHHA is conducted for three locations along the Atlantic coast of the USA, where NDBC buoys are located. The NOAA station IDs for the three sites are 44008, 44009 and 41008 (see Table 2). In this section, these sites are referred to by the postal abbreviation of their closest state, MA for 44008, DE for 44009 and GA for 41008. The first step in a POHHA is to develop a stochastic catalog of synthetic hurricanes for the location of interest (see Fig. 1). The specific stochastic catalog used here considers 100,000 years of hurricane activity in the Atlantic basin and was developed by Liu (2014). The numerical examples provided at the end of this paper are based on a sampling of 1000 hurricanes among the 100,000 years of hurricanes in the catalog. The sampling approach is outlined in Liu (2014) and includes two steps: First, the catalog is filtered to only include hurricanes

passing within 250 km of the considered location, and then, from this subset of hurricanes, 1000 hurricanes are selected based on a Latin hypercube approach (or inverse CDF approach) to find a set of hurricanes for each site that closely approximates the CDF based on the entire 100,000-year catalog. Using the stochastic catalog, a hurricane arrival rate can be calculated for each of the three sites. The rates differ significantly among the three sites with the GA site estimated to have hurricanes passing within 250 km most frequently at 1.16 year^{-1} and DE and MA estimated to have annual hurricane frequencies of 0.79 and 0.88 year^{-1}, respectively. Given the CDF value of a particular hazard intensity, $F_X(x)$, and the annual rate of hurricane occurrence, ν, the MRP of the hazard intensity is calculated as,

$$\mathrm{MRP} = \frac{1}{\nu(1 - F_X(x))} \tag{12}$$

For this example, 100 realizations of wind speeds and significant wave heights are sampled based on the WWPEs for each of the 1000 hurricanes considered at each site, and the results are presented in Fig. 11.

It can be seen from these figures that, in all cases, including uncertainty in the WWPEs causes a modest increase in the estimated intensity for MRPs > 10 years with the magnitude of the difference increasing with increasing MRP. The effect of including uncertainty is greater for the significant wave height than the wind speed, reflecting the larger variance observed in the wave height prediction. Numerical results of this comparison are summarized in Table 4, and the average increase in wind speed when considering uncertainty among all three sites for a 50-year MRP is 4.3 and 7.9 % for a 500-year MRP. The average increase in significant wave height when considering uncertainty is 8.0 % for a 50-year MRP and 18.7 % for a 500-year MRP.

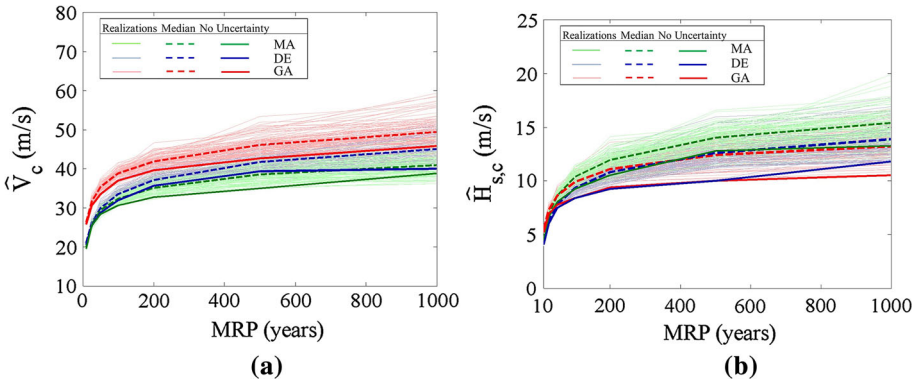

Fig. 11 Results from a POHHA for WWPEs with and without uncertainty for **a** sustained wind speeds $\hat{V}_c$ and **b** significant wave height $\hat{H}_{s,c}$. Thin *solid lines* indicate results from 100 realizations of $\hat{V}_c$ and $\hat{H}_{s,c}$ for each site with $\sigma_{\varepsilon_{V_c}} = 0.13$ and $\sigma_{\varepsilon_{H_{s,c}}} = 0.25$. *Bold solid lines* indicate the median of these realizations, while *bold dashed lines* indicate predicted values without consideration of uncertainty in the WWPEs (i.e., with $\sigma_{\varepsilon_{V_c}} = \sigma_{\varepsilon_{H_{s,c}}} = 0$)

Table 4 Wind speed and significant wave height for investigated sites for 50- and 500-year MRPs

Site	MRP (years)	Wind speed, $\hat{V}_c$ (m/s)			Significant wave height, $\hat{H}_{s,c}$ (m)		
		No uncertainty	Median	Difference %	No uncertainty	Median	Difference %
MA	50	28.4	29.4	3.4	8.1	8.6	6.2
	500	35.0	38.5	10.0	12.8	14.0	9.3
DE	50	28.8	30.0	4.2	5.5	5.9	6.7
	500	39.4	41.7	5.8	8.4	10.3	22.7
GA	50	33.6	35.4	5.3	7.8	8.6	11.1
	500	42.7	46.1	8.0	10.0	12.4	24.0

10 Conclusions

In this paper, probabilistic wind and wave prediction equations (WWPEs) are formulated using a statistical comparison between predictions of wind speed and significant wave height from simple parametric models (the Holland model for wind and Young's model for waves) and buoy measurements during Atlantic hurricanes. Such equations provide a useful tool to engineers quantifying hurricane risk to offshore structures as part of POHHA. During the formulation of the WWPEs, two biases in the parametric models are identified and corrected. The first bias relates to the uncertainty in the wind speed prediction as a function of wind speed magnitude, and the second bias relates to the uncertainty in the wave height prediction as a function of water depth. After correcting for these two biases, the probabilistic nature of the uncertainty in the model predictions is found to be reasonably characterized by a zero mean, normally distributed random variable representing the difference between logarithms of predictions and measurements. The uncertainty in wave height predictions with Young's model is found to be considerably greater than the uncertainty in wind speed predictions with the Holland model with the former having a standard deviation of the logarithmic difference between predictions and measurements of 0.25 and the latter having a standard deviation of 0.13. It is noted that the uncertainty associated with plus and minus one logarithmic standard deviation is 114 and 88 % of the expected values if the standard deviation is 0.13 and 128 and 78 % of the expected values if the standard deviation is 0.25. The impact of this degree of uncertainty is assessed by calculating hurricane wind speed and significant wave height at three sites for various MRPs and for two situations: with and without consideration of uncertainty in the WWPEs. The effect of including uncertainties in the estimation of hurricane-induced wind and waves is shown to increase the estimate of the wind speed and the significant wave height, especially for higher MRPs. The effect is more pronounced for estimating significant wave height than for wind speed on account of the greater uncertainty in the estimate of the significant wave height. Specifically, for the three sites, the median of the wind speed considering uncertainty increases by an average of 4.3 % for a 50-year MRP and 7.9 % for a 500-year MRP. For significant wave height, the median, considering uncertainty, increases by an average of 8.0 % for a 50-year MRP and 18.7 % for a 500-year MRP.

Acknowledgments This work is based upon work supported by the National Science Foundation under Grants CMMI-1234560 and CMMI-1234656, the Massachusetts Clean Energy Center, Northeastern University, and the University of Massachusetts, Amherst. Any opinions, findings and conclusions or

recommendations expressed in this material are those of the authors and do not necessarily reflect the view of the National Science Foundation or other funding agencies.

References

Baker JW (2013) An introduction to probabilistic seismic hazard analysis. White Pap 2(1):79

Batts ME, Simiu E, Russell LR (1980) Hurricane wind speeds in the United States. J Struct Div 106(10):2001–2016

Bender MA, Ginis I (2000) Real-case simulations of hurricane-ocean interaction using a high-resolution coupled model: effects on hurricane intensity. Mon Weather Rev 128(4):917–946

Booij N, Ris RC, Holthuijsen LH (1999) A third generation wave model for coastal regions: 1. Model description and validation. J Geophys Res Oceans 104(C4):7649–7666

Chawla A, Spindler DM, Tolman HL (2013) Validation of a thirty year wave hindcast using the Climate Forecast System Reanalysis winds. Ocean Model 70:189–206

Cornell CA (1964) Stochastic processes in civil engineering. Doctoral Dissertation, Stanford University, CA

Cornell CA (1968) Engineering seismic risk analysis. Bull Seismol Soc Am 58(5):1583–1606

Georgiou P (1985) Design wind speeds in tropical cyclone prone regions. Doctoral Dissertation, University of Western Ontario

Georgiou PN, Davenport AG, Vickery BJ (1983) Design wind speeds in regions dominated by tropical cyclones. J Wind Eng Ind Aerodyn 13(1):139–152

Holland GJ (1980) An analytic model of the wind and pressure profiles in hurricanes. Mon Weather Rev 108(8):1212–1218

Holland GJ, Belanger JI, Fritz A (2010) A revised model for radial profiles of hurricane winds. Mon Weather Rev 138(12):4393–4401

Huang Z, Rosowsky DV, Sparks PR (2001) Long-term hurricane risk assessment and expected damage to residential structures. Reliab Eng Syst Saf 74(3):239–249

Jayaram N, Baker J (2010) Probabilistic seismic lifeline risk assessment using efficient sampling and data reduction techniques. Doctoral Dissertation, Stanford University

Kerry E, Ravela S, Vivant E, Risi C (2006) A statistical deterministic approach to hurricane risk assessment. Bull Am Meteorol Soc 87:299–314

Liu F (2014) Projections of future U.S. design wind speeds and hurricane losses due to climate change. Doctoral Dissertation, Clemson University, Clemson

Luettich RA, Westerink JJ (2004) Formulation and numerical implementation of the 2D/3D ADCIRC finite element model version 44. XX (p 74). R. Luettich

Neumann C (1991) The National Hurricane Center Risk Analysis Program (HURISK)

Powell MD, Houston SH, Amat LR, Morisseau-Leroy N (1998) The HRD real-time hurricane wind analysis system. J Wind Eng Ind Aerodyn 77:53–64

Powell MD, Vickery PJ, Reinhold TA (2003) Reduced drag coefficient for high wind speeds in tropical cyclones. Nature 422:279–283

Russell LR (1971) Probability distributions for hurricane effects. J Waterw Harb C Eng Div 97(1):139–154

Saha S, Moorthi S, Pan H, Wu X, Wang J, Nadiga S, Tripp P, Kistler R, Wollen J, Behringer D, Liu H, Stokes D, Grumbine R, Gayno G, Wang J, Hou Y, Chuang H, Juang H, Sela J, Iredell M, Treadon R, Kleist D, VanDelst P, Keyser D, Derber J, Ek M, Meng J, Wei H, Yang R, Lord S, van den Dool H, Kumar A, Wang W, Long C, Chelliah M, Xue Y, Huang B, Schemm J, Ebisuzaki W, Lin R, Xie P, Chen M, Zhou S, Higgins W, Zou C, Liu Q, Chen Y, Han Y, Cucurull L, Reynolds R, Rutledge G, Goldberg M (2010) The NCEP climate forecast system reanalysis. Bull Am Meteorol Soc 91:1015–1057

Schwerdt RW, Ho FP, Watkins RW (1979) Meteorological criteria for standard project hurricane and probable maximum hurricane wind fields, Gulf and East Coasts of the United States. NOAA Technical Report NWS 23, US Department of Commerce, Washington, DC

Simiu E, Scanlan RH (1996) Wind effects on structures, 3d edn. Wiley, New York

Sparks PR, Huang Z (2001) Gust factors and surface-to-gradient wind speed ratios in tropical cyclones. J Wind Eng Ind Aerodyn 89:1058–1470

Tryggvason BV, Davenport AG, Surry D (1976) Predicting wind-induced response in hurricane zones. J Struct Div 102(12):2333–2350

Valamanesh V, Myers AT, Arwade SR (2015) Analysis of extreme metocean conditions for offshore wind turbines. Struct Saf 55:60–69

Vickery PJ, Twisdale LA (1995) Wind-field and filling models for hurricane wind-speed predictions. J Struct Eng 121(11):1700–1709
Vickery PJ, Wadhera D (2008a) Development of design wind speed maps for the Caribbean for application with the wind load provisions of ASCE 7. Pan American Health Organization, Washington, DC
Vickery PJ, Wadhera D (2008b) Statistical models of Holland pressure profile parameter and radius to maximum winds of hurricanes from flight-level pressure and H*Wind data. J Appl Meteorol Clim 47(10):2497–2517
Vickery P, Skerlj P, Steckley A, Twisdale L (2000a) Hurricane wind field model for use in hurricane simulations. J Struct Eng 126(10):1203–1221
Vickery PJ, Skerlj PF, Twisdale LA (2000b) Simulation of hurricane risk in the US using an empirical track model. J Struct Eng 126(10):1222–1237
Vickery PJ, Wadhera D, Twisdale LA, Lavelle FM (2009a) US hurricane wind speed risk and uncertainty. J Struct Eng 135(3):301–320
Vickery PJ, Wadhera D, Powell MD, Chen Y (2009b) A hurricane boundary layer and wind field model for use in engineering applications. J Appl Meteorol Clim 48(2):381–405
Vickery PJ, Masters FJ, Powell MD, Wadhera D (2009c) Hurricane hazard modeling: the past, present, and future. J Wind Eng Ind Aerodyn 97(7):392–405
Young IR (1988) Parametric hurricane wave prediction model. J Waterw Port C 114(5):637–652